

STRUCTURE OF MATTER
AND QUANTUM CHEMISTRY

Synthesis, Characterization, and Biological Investigation
of Alanine-Based Sulfonamide Derivative: FT-IR, ¹H NMR Spectra:
MEP, HOMO–LUMO Analysis, and Molecular Docking¹

Parvaneh Shafieyoon^{a,*}, Ebrahim Mehdipour^{a,**}, and Jacek Michalski^{b,***}

^aDepartment of Chemistry, Faculty of Science, Lorestan University, Khoramabad, Iran

^bDepartment of Bioorganic Chemistry, Faculty of Engineering and Economics, Wrocław University of Economics, Wrocław, Poland

*e-mail: parva127@yahoo.com, shafieyoon.pa@fs.lu.ac.ir

**e-mail: e_mehdipour@yahoo.com, mehdipour.e@lu.ac.ir

***e-mail: jacek.michalski@ue.wroc.pl

Received February 17, 2018; revised October 15, 2018; accepted January 15, 2019

Abstract—A combined experimental and theoretical investigation has been reported on *N*-(alanine)-*p*-styrene sulfonamide (abbreviated as ASS). The new title compound have been synthesized for the first time from the reaction of *p*-styrene sulfonyl chloride and (S)-alanine in the mild condition. The ASS was confirmed using FT-IR and ¹H-NMR spectra. IR and ¹H NMR spectrum, MEP and HOMO–LUMO analysis of the ASS have been investigated using DFT method. ¹H-NMR chemical shift values have been compared with experimental data. The potential energy distribution (PED) of the normal modes among the respective internal coordinates have been calculated for ASS using the BALGA program and compared with theoretical and experimental values. The ASS is investigated against *Staphylococcus aureus* and *Escherichia coli*. Molecular Docking study has also been reported.

Keywords: *N*-(alanine)-*p*-styrene sulfonamide, (S)-alanine, DNA, BSA, molecular docking, MEP, HOMO and LUMO analysis

DOI: 10.1134/S0036024419070215

INTRODUCTION

Sulfonamide compounds, as antibacterial agents, are extensively used in the world because of their low toxicity and excellent activity against bacterial diseases. These materials are widely used to treat many types of infections caused by bacteria and prevent the growth of bacteria in the body. Some sulfonamide derivatives in pharmaceutical as antibacterial agents such as imidazole and benzimidazole sulfonamides [1–3] and as antiviral agents such as *Trypanosoma brucei* *N*-Myristoyltransferase inhibitor have been applied [4, 5]. In the final, antimicrobial properties of Sulfonamide derivatives are well known. In the pioneering research, relationships between the degree of ionization in the sulfonamides and bacterial activity have been reported [6, 7]. The number of sulfonamide derivatives as an inhibitor to prevent from generation and progression of cancer cells were applied such as tetrahydroquinoline and chromone containing sulfonamide moiety [8–11] and excellent cytotoxic effects against breast cancer cells was also reported

[12]. Some people have diabetes mellitus. It is an inveterate disease leading to the increase concentrations of glucose in blood which is called hyperglycemia [13]. Pyridine-based sulfonamide as organic molecule for the potential treatment of type-II diabetes mellitus was reported [14]. This type of compounds were widely used to control blood glucose levels of patients [15, 16]. During the past two decades, the synthesis of sulfonamide derivatives have been developed as antibacterial and anticancer drugs [17–19]. These results promoted us to synthesize and evaluate a new series of sulfonamide derivatives for pharmaceutical chemistry, we have selected an amino acid and styrene structural parts to prepare a new sulfonamide structure due to the major importance of these group in coordination to metals and synthesis of novel complex-based sulfonamide drugs. In our previous research, we reported the synthesis of sulfonamide and amino acid derivatives [20, 21] and theoretical investigation about the new drug-based material. In this work, the title compound was obtained by the reaction of amino acid with para-styrene sulfonyl chloride. The bioactivity of this compound for the first time was investigated in vitro

¹ The article is published in the original.

against gram positive and gram negative bacteria. Molecular docking calculations were performed to evaluate the medicinal properties of the title compound as anticancer.

EXPERIMENTAL

Material and Methods

p-Styrene sulfonic acid sodium salt, PCl_5 , sodium hydroxide, and (S)-(+)-alanine were purchased from Merck and Sigma–Aldrich companies and were used without further purification. Fourier transform infrared (FT-IR) spectra of prepared compounds were recorded at 400–4000 cm^{-1} region using KBr pellets on Shimadzu FT-IR 8400 spectrometer. ^1H NMR spectrum was recorded on a Bruker Ultrashield 400 MHz spectrometer using D_2O as solvent.

Preparation of *p*-Styrene Sulfonyl Chloride

To prepare the monomer first, *p*-styrene sulfonyl chloride was synthesized as follows: *p*-styrene sulfonyl chloride was synthesized by the reaction of 5.00 g of *p*-styrene sulfonic acid sodium salt with 7.50 g of PCl_5 , as chlorination agent. The product was separated from inorganic materials by chloroform and ice water. The chloroform was evaporated from the *p*-styrene sulfonyl chloride. Experimental details are described in [22].

Preparation of *N*-(Alanine)-*p*-Styrene Sulfonyl Chloride (ASS)

The synthetic method for the preparation of the ASS with chemical formula ($\text{C}_{11}\text{H}_{13}\text{NO}_4\text{S}$) is as follows: in a 100 mL round-bottomed flask, equipped with magnetic stirrer, 4.86 g *p*-styrene sulfonyl chloride (24 mmol) in 50 mL CHCl_3 as a solvent and 2.14 g (S)-(+)-alanine (24 mmol) were placed. Then, 2.4 mL NaOH 1M was slowly added. The reaction mixture was stirred for 4 h at room temperature. After the reaction time, the solvent was evaporated and ASS as the product was obtained. The obtained product was washed 3 times with water and analyzed without further purification (yield 5.20 g, 85.0%; m.p. 123°C).

FT-IR (KBr, cm^{-1}): 3620, 3460, 3267, 3096, 2941, 2837, 1712, 1651, 1595, 1425, 1344, 1228, 1157, 1091, 1053.

^1H -NMR (D_2O , ppm): 1.42 (CH_3), 3.97 (CH), 4.70 (NH) 5.42 (CH in vinyl), 5.92 (CH in vinyl), 6.77 (CH in vinyl), 7.59 (CH benzene), 7.75 (CH benzene), 9.96 (COOH).

Computational Details

Calculations of the ASS were performed using Gaussian 09 software [23]. The calculations including geometry optimization(opt-freq), MEP, HOMO–

LUMO analysis, and IR and ^1H NMR spectrum were performed by using density functional theory (DFT) [24]. The optimization of the title compound was carried out using CAM-B3LYP method Aug.-cc-pVDZ [25] basis set, and ^1H NMR spectra using B3LYP/6-311+g(*d,p*). The RMS error value was calculated for ^1H NMR spectrum using the following expression [26]:

$$\text{RMS} = \sqrt{\frac{1}{n-1} \sum_i^n (v_i^{\text{calc}} - v_i^{\text{exp}})^2}$$

For calculating the simulated vibrational spectra B3LYP/6-311g(2*d*,2*p*) was used. The potential energy distribution (PED) of the normal modes among the respective internal coordinates was calculated for ASS using the BALGA program [27] and compared with theoretical and experimental values. PASS (Prediction of Activity Spectra) technique was applied as an online tool to predict the activity of compound [28]. The ASS (*N*-alanine *p*-styrene sulfonyl chloride) as a ligand, was optimized by using CAM-B3LYP method Aug –cc–pVDZ basis set and prepared for docking. The 3D crystal structure of employed DNA and BSA were obtained from Protein Data Bank (PDB ID: 423D, 4F5S). Molecular docking is an important tool to get an insight into ligand–receptor interaction and to screen molecule for the binding affinities against a selected receptor. All molecular docking calculations were performed on AutoDock-Vina software [29]. As the most popular algorithm, Lamarckian Genetic Algorithm (LGA), available in Autodock was employed for docking [30, 31]. The graphical representation of ligand-DNA and ligand-BSA interaction was obtained using ligplot software [32].

Antibacterial Assays

The minimal inhibitory concentration (MIC) of the ASS as antibacterial agent against *Escherichia coli* and *Staphylococcus aureus* will be reported in the next section. The ASS was tested for its antimicrobial activity against *Staphylococcus aureus*, as the model from Gram-positive and *Escherichia coli* as Gram-negative bacteria by the disk diffusion method [33].

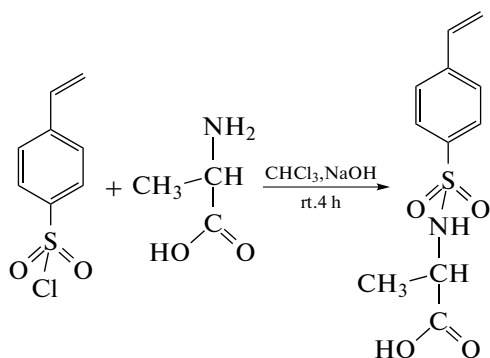
Preparation of Nutrient-Agar Medium

For this work, 3.80 g of Nutrient-Agar (NA) medium was dissolved in 100 mL of distilled water. This solution was sterilized at 120°C for 20 min in an autoclave. Then, 20 mL of this solution was solidified in Petri plate.

RESULT AND DISCUSSION

Synthesis and Characterization

ASS was prepared by reactions of *p*-styrene sulfonyl chloride with (S)-alanine in the presence of CHCl_3 as



Scheme 1. The reaction involving synthesis of ASS.

a solvent and NaOH (Scheme 1). The new ligand was characterized by FT-IR and ^1H NMR spectroscopy (data in the experimental section).

Tautomeric and Dynamic Processes

ASS can be presented in two different tautomers (named as T_1 , T_2). It is important to be conscious of the relative stabilities of these tautomers (Fig. 1).

In fact, structures of these tautomers were calculated using CAM-B3LYP/Aug-cc-pVDZ level of theory. Thermodynamic properties such as HF energies, relative enthalpies, relative total energies and relative Gibbs free energies for three Tautomers (T_1 and

T_2) are shown in the Table 1. As a result, T_1 tautomer is more stable due to the symmetrical elements in SO_2 .

Solvent Effects (ASS Model)

The effect of solvent is approximated by using the self-consistent reaction field method based on the ASS model. In this case, only the effect of the polarity of solvent on the energy and dipole moment kinetics of the T_1 is studied. Four solvents with different polarities (water, heptane, nujol and acetonitrile) have been considered to investigate their effect on the T_1 . The results of these effects on kinetic and thermodynamic parameters for T_1 are listed in Table 2. Since T_1 has the minimum dipole moment in nujol and maximum in water as a solvent, the results sustain, it is undergo its stability.

Molecular Structural

The optimized geometry (opt-freq) using (CAM-B3LYP method Aug-cc-pVDZ) of ASS was calculated. The numbers of atoms was defined in Fig. 2.

Spectroscopic Characterization of ASS

In the DFT calculations the molecular energies were calculated for all possible conformations of the studied compound (Fig. 3).

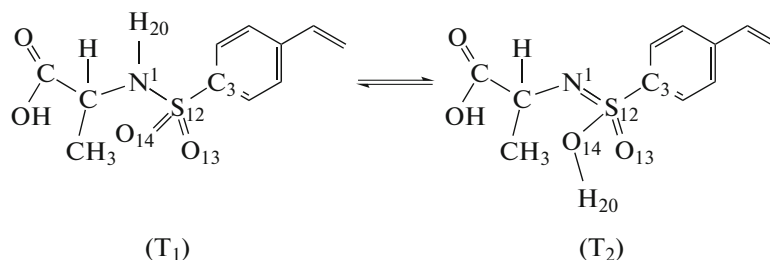


Fig. 1. The general structures of ASS tautomers.

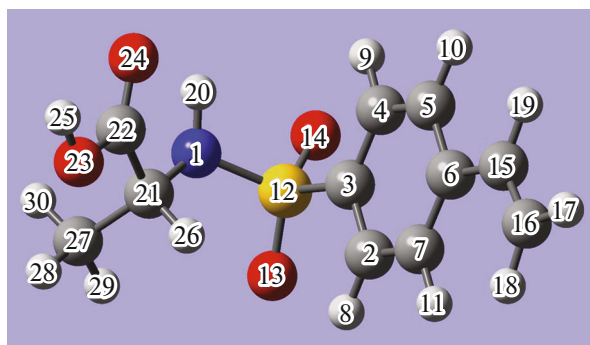


Fig. 2. (Color online) Optimized geometry (CAM-B3LYP method Aug-cc-pVDZ) of ASS.

Table 1. Kinetic and thermodynamic data of two tautomers

Tautomer	E_e	ZPE	Rel. E	Rel. H_{298}°	Rel. G_{298}°
T ₁	-1180.5157	0.2335	-1180.2912	-1180.2735	-1180.3386
T ₂	-1180.4285	0.2305	-1180.2068	-1180.1886	-1180.2534

All energetic data have been reported in Hartree.

Table 2. Effect of solvent data of T₁

Value	Isolated	Acetonitrile	Heptane	Nujol	Water
$E(\text{RB+HF-LYP})$	-1181.06482596	-1181.09216133	-1181.03365219	-1181.09346740	-1180.53215999
Dipole moment	6.5689	6.5689	6.5689	6.5600	7.3644T ₁

The potential energy curves as a function of the torsion angles around the S–N bond was shown. In addition, for a rotamer with the lowest energy, it is possible to have a hydrogen bond with two donors, which would further stabilize the system (C21–H26···O13 and C2–H8···O13). The intermolecular hydrogen bonds play a greater role, as can be seen on the experimental spectrum. The experimental FT-IR of ASS are reported above (Fig. 4), while the computed values for the two most stable rotamers along with the potential energy distribution are shown in Table 3. The bolded

fragments refer to the differences in the band position, intensity, as well as the differences in the PED. The calculated intensity of the 55 band for a rotamer with a rational CSNC angle of -64° is very strong, as in the experimental spectrum. This may prove more favored for this conformation. The theoretical spectrum has been rescaled.

A scaling factor of 0.954 was used for the all spectral range (Table 3). The C–H stretching frequencies of aromatic can be observed in the range of 3100–3000 cm^{-1} , is showed at 3096 cm^{-1} (calculated values

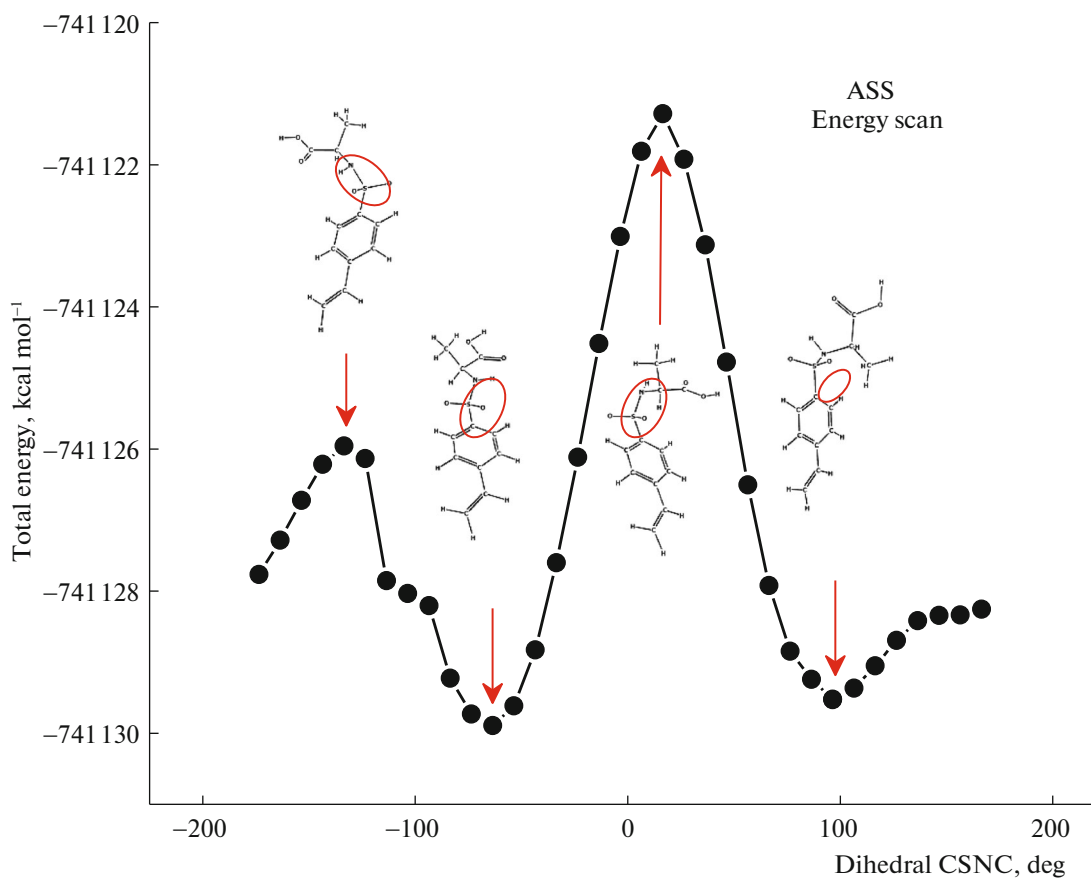


Fig. 3. (Color online) The potential energy curve of the S–N-bond in ASS as a function of the torsion C21–N–S–C2 angle.

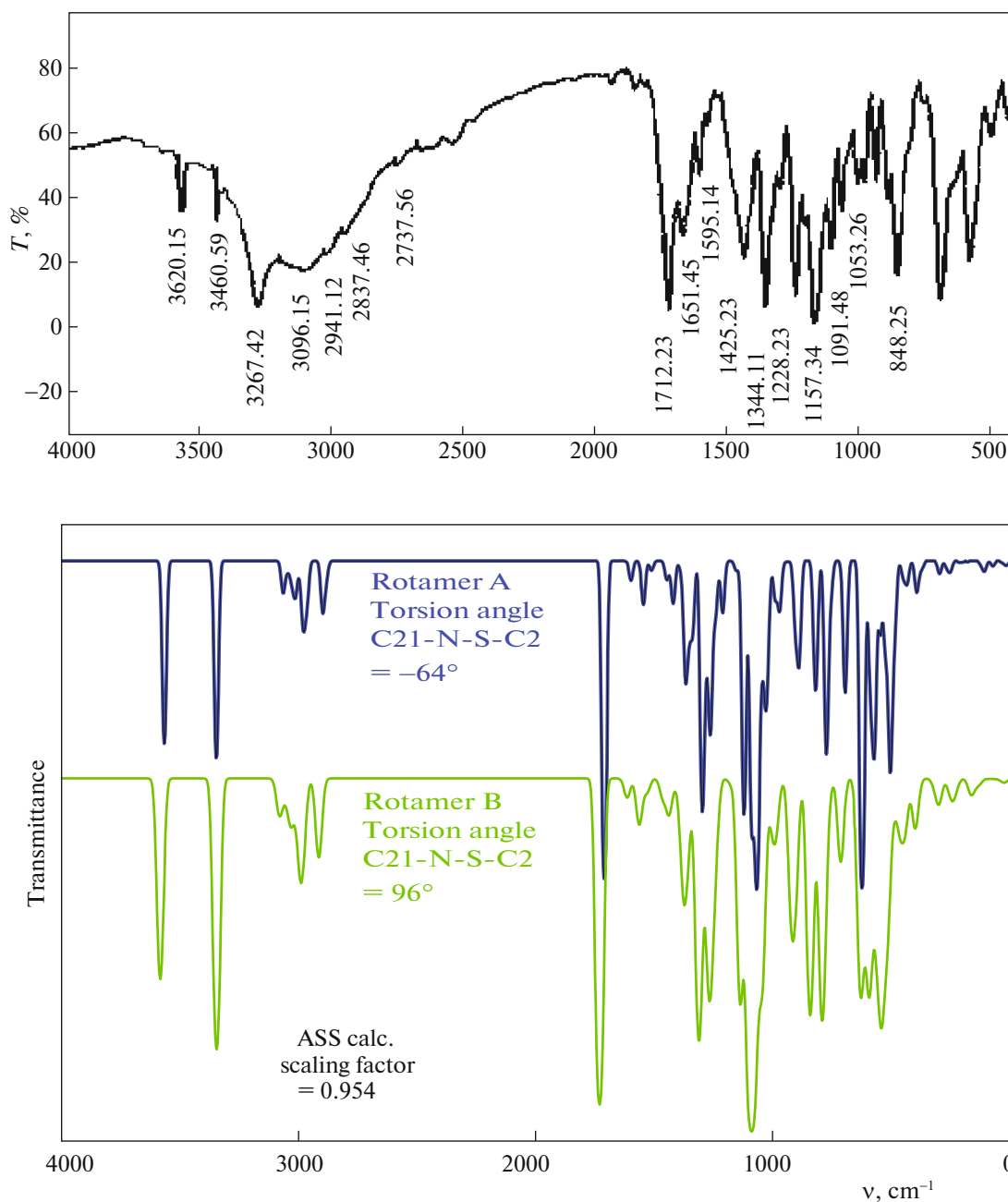


Fig. 4. (Color online) The experimental (top) and calculated (bottom) FT-IR spectra of ASS.

are present in the range of $3066\text{--}3029\text{ cm}^{-1}$. The aliphatic C–H stretching frequencies are also appeared below 3000 cm^{-1} (calc. $3082\text{--}2900\text{ cm}^{-1}$). The C=C and aromatic stretching vibration in the range of $1650\text{--}1400\text{ cm}^{-1}$ (calc. $1614\text{--}1368\text{ cm}^{-1}$) and the C–H bending bands are appeared in the regions $1450\text{--}1000\text{ cm}^{-1}$ (in-plane C–H bend) (calc. $1462\text{--}1005\text{ cm}^{-1}$). In addition, the stretching mode of NH group is appeared at 3460 cm^{-1} (calc. 3364 cm^{-1}). In the following discussion, sulfonamides absorb strongly at $1370\text{--}1335$ and $1170\text{--}1155\text{ cm}^{-1}$. The stretching mode symmetrical and asymmetrical

O=S=O is observed at 1157 cm^{-1} (calc. 1103 cm^{-1}) and $1344\text{--}1284\text{ cm}^{-1}$ (calc. $1313\text{--}1279\text{ cm}^{-1}$), respectively. The C=O stretching frequency is shown at 1712 cm^{-1} (calc. 1727 cm^{-1}).

Observed and Calculated ^1H NMR Chemical Shifts

The experimental ^1H -NMR spectrum of the compound are reported above (Fig. 5). The ^1H -NMR spectrum of the ASS was recorded in D_2O as solvent with TMS as internal standard at 400 MHz.

Table 3. Theoretical (B3LYP/6-311G(2d,2p)) and experimental IR wavenumbers with PEDs of the ASS vibrations for the two most stable rotamers

No.	$\nu_{\text{exp}}, \text{cm}^{-1}$	Torsion angle C21–N–S–C2 = -64°		Torsion angle C21–N–S–C2 = 96°	
		$\nu_{\text{calc}}, \text{cm}^{-1}$ (IR abs., %)	PED, %	$\nu_{\text{calc}}, \text{cm}^{-1}$ (IR abs., %)	PED, %
1	3620w	3583(30)	$\nu\text{OH} - 100$	3583(35)	$\nu\text{OH} - 100$
2	3460w	3363(34)	$\nu\text{NH} - 100$	3346(60)	$\nu\text{NH} - 99$
3	3267s	3082(4)	$\nu\text{CH}_{\text{Vi}} - 99$	3081(4)	$\nu\text{CH}_{\text{Vi}} - 99$
4		3066(1)	$\nu\text{CH}_\phi - 90$	3067(1)	$\nu\text{CH}_\phi - 99$
5	3095m	3057(1)	$\nu\text{CH}_\phi - 99$	3061(1)	$\nu\text{CH}_\phi - 99$
6		3044(2)	$\nu\text{CH}_\phi - 98$	3043(2)	$\nu\text{CH}_\phi - 99$
7		3029(4)	$\nu\text{CH}_\phi - 99$	3029(5)	$\nu\text{CH}_\phi - 99$
8		3007(2)	$\nu\text{CH}_{\text{Vi}} - 94$	3006(2)	$\nu\text{CH}_{\text{Vi}} - 98$
9		2996(5)	$\nu\text{CH}_{\text{Vi}} - 100$	2996(5)	$\nu\text{CH}_{\text{Vi}} - 100$
10		2995(3)	$\nu\text{CH}_{\text{Me}} - 100$	2988(7)	$\nu\text{CH}_{\text{Me}} - 100$
11	2941m	2981(5)	$\nu\text{CH}_{\text{Me}} - 100$	2977(5)	$\nu\text{CH}_{\text{Me}} - 100$
12	2855sh	2915(6)	$\nu\text{CH}_{\text{Me}} - 97$	2918(5)	$\nu\text{CH}_{\text{C}\alpha} - 80 + \nu\text{CH}_{\text{Me}} - 20$
13	2834w	2900(2)	$\nu\text{CH} - 96$	2912(6)	$\nu\text{CH}_{\text{Me}} - 81 + \nu\text{CH}_{\text{C}\alpha} - 18$
14	1712vs	1727(91)	$\nu\text{CO} - 86 + \delta\text{CO} - 5$	1730(100)	$\nu\text{CO} - 86$
15	1654m	1614(2)	$\nu\text{C}=\text{C}_{\text{Vi}} - 64 + \delta\text{CH}_{\text{Vi}} - 28 + \nu\text{CCH}_3 - 5$	1613(2)	$\nu\text{C}=\text{C}_{\text{Vi}} - 62 + \delta\text{CH}_{\text{Vi}} - 26$
16	1595v	1561(6)	$\nu\phi - 63 + \delta\text{CH}_\phi - 23 + \delta\phi - 10$	1563(6)	$\nu\phi - 66 + \delta\text{CH}_\phi - 23 + \delta\phi - 10$
17	1566vw	1527(1)	$\nu\phi - 69 + \delta\text{CH}_\phi - 12 + \delta\phi - 8$	1529(2)	$\nu\phi - 78 + \delta\text{CH}_\phi - 13$
18	1465sh	1462(2)	$\delta\text{CH}_\phi - 61 + \nu\phi - 32$	1463(2)	$\delta\text{CH}_\phi - 52 + \nu\phi - 31$
19		1439(2)	$\delta\text{CH}_3 - 94$	1440(2)	$\delta\text{CH}_3 - 92$
20	1425m	1434(4)	$\delta\text{CH}_3 - 91$	1434(3)	$\delta\text{CH}_3 - 100$
21	1399sh	1402(1)	$\delta\text{CH}_{\text{Vi}} - 82 + \nu\phi - 5$	1401(1)	$\delta\text{CH}_{\text{Vi}} - 84$
22		1383(17)	$\delta\text{NH} - 42 + \delta\text{CH}_{\text{C}\alpha} - 20 + \delta\text{CH}_3 - 19 + \nu\text{CC}_{\text{COOH}} - 5$	1378(10)	$\delta\text{NH} - 40 + \delta\text{CH}_{\text{C}\alpha} - 20 + \delta\text{CH}_3 - 15$
23		1368(8)	$\nu\phi - 42 + \delta\text{CH}_\phi - 39 + \delta\text{CH}_{\text{Vi}} - 9$	1368(8)	$\nu\phi - 43 + \delta\text{CH}_\phi - 38$
24		1353(9)	$\delta\text{CH}_3 - 83 + \delta\text{NH} - 5$	1355(5)	$\delta\text{CH}_3 - 89$
25	1344vs	1313(50)	$\delta\text{CO} - 29 + \nu\text{SO} - 19 + \delta\text{CH}_3 - 14 + \delta\text{NH} - 13 + \nu\text{CH}_{\text{Me}} - 11 + \nu\text{CC}_{\text{COOH}} - 5 + \delta\text{CH}_{\text{C}\alpha} - 5$	1311(55)	$\delta\text{CO} - 34 + \delta\text{NH} - 14 + \nu\text{CH}_{\text{Me}} - 12 + \delta\text{CH}_3 - 12 + \nu\text{SO} - 12$
26		1296(4)	$\delta\text{CH}_{\text{Vi}} - 42 + \delta\text{CH}_\phi - 23 + \nu\text{C}=\text{C}_{\text{Vi}} - 13 + \nu\phi - 8$	1295(1)	$\delta\text{CH}_{\text{Vi}} - 49 + \delta\text{CH}_\phi - 24 + \nu\text{C}=\text{C}_{\text{Vi}} - 15 + \nu\phi - 10$
27		1294(6)	$\delta\text{CH}_{\text{C}\alpha} - 61 + \delta\text{CO} - 9 + \nu\text{SO} - 7$	1288(1)	$\delta\text{CH}_{\text{C}\alpha} - 79$
28	1284vw	1279(26)	$\nu\text{SO} - 53 + \delta\text{NH} - 14 + \delta\text{CH}_{\text{C}\alpha} - 14$	1273(0)	$\delta\text{CH}_\phi - 57 + \nu\phi - 22 + \delta\text{CH}_{\text{Vi}} - 16$
29		1272(2)	$\delta\text{CH}_\phi - 59 + \nu\phi - 20 + \delta\text{CH}_{\text{Vi}} - 11$	1269(31)	$\nu\text{SO} - 56 + \delta\text{CH}_{\text{C}\alpha} - 14$
30		1257(7)	$\nu\phi - 64 + \delta\text{CC}_{\text{Vi}} - 12 + \delta\text{CH}_{\text{Vi}} - 7 + \nu\text{SO} - 5$	1256(14)	$\nu\phi - 55 + \nu\text{SO} - 13 + \delta\text{CH}_{\text{Vi}} - 18$
31	1228s	1227(7)	$\delta\text{CH}_{\text{C}\alpha} - 56 + \delta\text{NH} - 14 + \delta\text{CO} - 14 + \delta\text{CH}_3 - 8$	1239(7)	$\delta\text{CH}_{\text{C}\alpha} - 49 + \delta\text{NH} - 20 + \delta\text{CO} - 13 + \nu\text{SO} - 11$
32	1190w	1170(1)	$\nu\phi - 30 + \nu\text{CCH}_3 - 29 + \delta\text{CH}_\phi - 18 + \delta\phi - 10 + \delta\text{CH}_{\text{Vi}} - 9$	1173(1)	$\nu\phi - 38 + \nu\text{CCH}_3 - 28 + \delta\text{CH}_\phi - 20 + \delta\text{CH}_{\text{Vi}} - 10$
33		1155(0)	$\delta\text{CH}_\phi - 70 + \nu\phi - 22$	1154(0)	$\delta\text{CH}_\phi - 69 + \nu\phi - 25$
34		1136(52)	$\delta\text{CO} - 25 + \nu\text{CH}_{\text{Me}} - 24 + \delta\text{CH}_{\text{C}\alpha} - 16 + \nu\text{NC} - 12 + \delta\text{CH}_3 - 7$	1136(42)	$\delta\text{CO} - 36 + \nu\text{CH}_{\text{Me}} - 32 + \delta\text{CH}_{\text{C}\alpha} - 16 + \nu\text{NC} - 12$
35	1157vs	1103(58)	$\nu\text{SO} - 64 + \nu\phi - \text{S} - 7 + \nu\phi - 8$	1097(80)	$\nu\text{SO} - 46 + \nu\phi - \text{S} - 22 + \delta\text{CH}_\phi - 14$

Table 3. (Contd.)

No.	$\nu_{\text{exp}}, \text{cm}^{-1}$	Torsion angle C21–N–S–C2 = -64°		Torsion angle C21–N–S–C2 = 96°	
		$\nu_{\text{calc}}, \text{cm}^{-1}$ (IR abs., %)	PED, %	$\nu_{\text{calc}}, \text{cm}^{-1}$ (IR abs., %)	PED, %
36		1090(1)	$\delta\text{CH}_\phi - 52 + \nu\phi - 37$	1085(46)	$\delta\text{CH}_\phi - 33 + \nu\phi - 26 + \delta\text{CH}_3 - 15$
37	1091m	1083(100)	$\nu\text{NC} - 27 + \nu\text{CH}_{\text{Me}} - 21 + \delta\text{CH}_3 - 23 + \delta\text{CO} - 7$	1082(61)	$\nu\text{NC} - 20 + \delta\text{CH}_3 - 17 + \nu\text{CH}_{\text{Me}} - 15 + \nu\phi - 14$
38		1063(13)	$\delta\text{CH}_3 - 37 + \nu\text{CC}_{\text{Me}} - 32 + \delta\text{CH}_{\text{C}\alpha} - 15 + \nu\text{NC} - 7 + \gamma\text{CO} - 6$	1061(14)	$\delta\text{CH}_3 - 41 + \nu\text{CC}_{\text{Me}} - 30 + \delta\text{CH}_{\text{C}\alpha} - 14$
39	1053w	1046(18)	$\nu\phi - 47 + \nu\text{SO} - 19 + \delta\text{CH}_\phi - 11 + \nu\phi - \text{S} - 9$	1045(26)	$\nu\text{SO} - 41 + \nu\phi - 38$
40		1036(8)	$\delta\text{CH}_3 - 39 + \delta\text{CH}_{\text{C}\alpha} - 22 + \nu\text{NC} - 11 + \nu\text{CC}_{\text{Me}} - 5 + \gamma\text{CO} - 5$	1039(8)	$\delta\text{CH}_3 - 49 + \delta\text{CH}_{\text{C}\alpha} - 21 + \nu\text{NC} - 12$
41		1005(5)	$\delta\text{CH}_{\text{Vi}} - 77 + \nu\phi - 19$	1004(5)	$\delta\text{CH}_{\text{Vi}} - 76 + \nu\phi - 17$
42	991vw	989(1)	$\delta\phi - 57 + \nu\phi - 30 + \delta\text{CH}_\phi - 11$	989(1)	$\delta\phi - 54 + \nu\phi - 31 + \delta\text{CH}_\phi - 10$
43	966vw	986(5)	$\gamma\text{CC}_{\text{Vi}} - 50 + \gamma\text{CH}_{\text{Vi}} - 46$	985(5)	$\gamma\text{CH}_{\text{Vi}} - 75 + \gamma\text{CC}_{\text{Vi}} - 21$
44		960(0)	$\gamma\text{CC}_{\text{Vi}} - 50 + \gamma\text{CH}_\phi - 25 + \gamma\phi - 17 + \gamma\text{CS} - 5$	955(0)	$\gamma\text{CH}_\phi - 82 + \gamma\phi - 16$
45		945(0)	$\gamma\text{CH}_\phi - 36 + \gamma\text{CS} - 33 + \gamma\phi - 27 + \gamma\text{CC}_{\text{Vi}} - 5$	945(0)	$\gamma\text{CH}_\phi - 68 + \gamma\phi - 30$
46	921vw	920(8)	$\nu\text{CC}_{\text{Me}} - 22 + \nu\text{SN} - 20 + \nu\text{NC} - 19 + \delta\text{CH}_3 - 16 + \nu\text{CC}_{\text{COOH}} - 7$	920(19)	$\nu\text{SN} - 21 + \nu\text{NC} - 19 + \nu\text{CC}_{\text{Me}} - 18 + \delta\text{CH}_3 - 18$
47	875vw	904(14)	$\gamma\text{CC}_{\text{Vi}} - 98$	902(14)	$\gamma\text{CC}_{\text{Vi}} - 98$
48	842s	837(11)	$\nu\text{SN} - 21 + \delta\text{CH}_3 - 18 + \nu\text{CC}_{\text{Me}} - 15 + \delta\text{NH} - 13 + \gamma\text{NH} - 8 + \delta\text{CH}_{\text{C}\alpha} - 10$	842(39)	$\delta\text{CH}_3 - 20 + \nu\text{CC}_{\text{Me}} - 17 + \nu\text{SN} - 18 + \delta\text{NH} - 16$
49		831(9)	$\gamma\text{CH}_\phi - 46 + \gamma\phi - 25 + \gamma\text{CC}_{\text{Vi}} - 20 + \gamma\text{CS} - 5$	834(11)	$\gamma\text{CH}_\phi - 64 + \gamma\phi - 21 + \gamma\text{CC}_{\text{Vi}} - 12$
50		815(0)	$\gamma\text{CH}_\phi - 54 + \gamma\text{CS} - 28 + \gamma\text{CC}_{\text{Vi}} - 17$	809(1)	$\gamma\text{CH}_\phi - 94$
51	798sh	789(33)	$\nu\text{CC}_{\text{COOH}} - 33 + \delta\text{CH}_3 - 14 + \nu\text{SN} - 13 + \nu\text{CH}_{\text{Me}} - 11 + \gamma\text{CO} - 6$	790(47)	$\nu\text{CC}_{\text{COOH}} - 31 + \delta\text{CH}_3 - 16 + \gamma\text{CO} - 14 + \nu\text{SN} - 10 + \nu\text{CH}_{\text{Me}} - 10$
52		771(4)	$\nu\phi - 30 + \delta\phi - 27 + \nu\text{CCH}_3 - 17 + \nu\phi - \text{S} - 5 + \delta\text{CH}_{\text{Vi}} - 5$	768(3)	$\nu\phi - 28 + \delta\phi - 27 + \nu\text{CCH}_3 - 19$
53	741vw	734(0)	$\gamma\phi - 46 + \gamma\text{CH}_\phi - 18 + \gamma\text{CS} - 16 + \gamma\text{CH}_{\text{Vi}} - 10 + \gamma\text{CC}_{\text{Vi}} - 7$	736(0)	$\gamma\phi - 45 + \gamma\text{CH}_\phi - 32 + \gamma\text{CC}_{\text{Vi}} - 17$
54		710(20)	$\gamma\text{CO} - 51 + \gamma\text{COOH} - 20 + \nu\text{CC}_{\text{Me}} - 14 + \delta\text{CH}_{\text{C}\alpha} - 9$	712(11)	$\gamma\text{CO} - 55 + \gamma\text{COOH} - 15$
55	676vs	639(99)	$\delta\text{SO}_2 - 32 + \gamma\text{NH} - 13 + \nu\phi - \text{S} - 12 + \delta\phi - 8 + \nu\text{CCH}_3 - 7$	632(16)	$\gamma\text{CC}_{\text{Vi}} - 25 + \delta\text{SO}_2 - 18 + \gamma\phi - 14 + \gamma\text{CH}_\phi - 10$
56		629(6)	$\gamma\text{CC}_{\text{Vi}} - 30 + \gamma\text{CH}_{\text{Vi}} - 25 + \gamma\phi - 20 + \gamma\text{CH}_\phi - 13$	626(21)	$\gamma\text{CC}_{\text{Vi}} - 26 + \delta\phi - 14 + \delta\text{SO}_2 - 11$
57		622(1)	$\delta\phi - 79 + \nu\phi - 11$	621(3)	$\delta\phi - 71 + \nu\phi - 11$
58	609sh	603(18)	$\delta\text{CO} - 37 + \gamma\text{COOH} - 23 + \nu\text{CH}_{\text{Me}} - 5$	602(10)	$\delta\text{CO} - 40 + \nu\text{SN} - 12 + \delta\text{SO}_2 - 10$
59		587(32)	$\gamma\text{NH} - 21 + \delta\phi - 11 + \gamma\text{COOH} - 9 + \delta\text{CH}_{\text{C}\alpha} - 8 + \gamma\text{SN} - 6 + \nu\phi - \text{S} - 5 + \nu\text{SN} - 5 + \delta\text{NH} - 5$	590(31)	$\gamma\text{NH} - 27 + \gamma\text{COOH} - 14 + \delta\text{COOH} - 12 + \delta\text{CH}_{\text{C}\alpha} - 11$
60		562(10)	$\gamma\text{COOH} - 51 + \delta\text{CO} - 13 + \gamma\text{CO} - 9 + \delta\text{CH}_{\text{C}\alpha} - 6 + \nu\text{CC}_{\text{Me}} - 5 + \gamma\text{NH} - 5$	562(20)	$\gamma\text{COOH} - 79$
61		539(12)	$\delta\text{SO}_2 - 38 + \delta\text{CC}_{\text{Vi}} - 21 + \delta\phi - 18 + \delta\text{COOH} - 6$	540(43)	$\delta\text{SO}_2 - 40 + \delta\phi - 14 + \delta\text{CC}_{\text{Vi}} - 14$

Table 3. (Contd.)

No.	$\nu_{\text{exp}}, \text{cm}^{-1}$	Torsion angle C21–N–S–C2 = -64°		Torsion angle C21–N–S–C2 = 96°	
		$\nu_{\text{calc}}, \text{cm}^{-1}$ (IR abs., %)	PED, %	$\nu_{\text{calc}}, \text{cm}^{-1}$ (IR abs., %)	PED, %
62	567s	519(37)	$\delta\text{SO}_2 - 48 + \gamma\phi - 11 + \gamma\text{CH}_\phi - 9 + \delta\text{CO} - 7$	515(23)	$\delta\text{SO}_2 - 50 + \delta\text{COOH} - 13$
63	482vw	501(9)	$\delta\text{SO}_2 - 34 + \delta\text{COOH} - 13 + \gamma\text{NH} - 14 + \gamma\text{SN} - 10$	487(4)	$\delta\text{SO}_2 - 23 + \gamma\text{NH} - 17 + \delta\text{CC}_{\text{Vi}} - 16 + \gamma\phi - 10$
64	474vw	464(2)	$\delta\text{CC}_{\text{Vi}} - 44 + \delta\text{SO}_2 - 15 + \delta\phi - 13 + \nu\text{CCH}_3 - 9 + \nu\phi - \text{S} - 5$	461(6)	$\delta\text{CC}_{\text{Vi}} - 33 + \gamma\phi - 19 + \delta\text{SO}_2 - 14$
65	423vw	448(3)	$\delta\text{SO}_2 - 34 + \gamma\phi - 31 + \gamma\text{CC}_{\text{Vi}} - 7 + \gamma\text{CS} - 5$	440(6)	$\delta\text{SO}_2 - 38 + \gamma\text{NH} - 20 + \gamma\phi - 14$
66		408(4)	$\delta\text{CH}_{\text{C}\alpha} - 38 + \gamma\phi - 13 + \delta\text{SO}_2 - 8 + \delta\text{COOH} - 7 + \delta\text{NH} - 7$	399(5)	$\delta\text{CH}_{\text{C}\alpha} - 36 + \gamma\phi - 20 + \gamma\text{CC}_{\text{Vi}} - 11 + \delta\text{SO}_2 - 10$
67		396(0)	$\gamma\phi - 79 + \gamma\text{CH}_\phi - 15$	395(1)	$\gamma\phi - 72 + \gamma\text{CH}_\phi - 12$
68		385(1)	$\delta\text{SO}_2 - 39 + \delta\text{CS} - 16 + \delta\text{COOH} - 11 + \delta\text{CC}_{\text{Vi}} - 8 + \gamma\phi - 6$	384(0)	$\delta\text{SO}_2 - 39 + \delta\text{COOH} - 17 + \delta\text{CS} - 15$
69		313(1)	$\gamma\text{CH}_\phi - 31 + \delta\text{SO}_2 - 19 + \delta\text{CH}_{\text{C}\alpha} - 16 + \nu\text{SN} - 6$	321(0)	$\delta\text{SO}_2 - 25 + \delta\text{CH}_{\text{C}\alpha} - 21 + \nu\text{SN} - 15$
70		310(1)	$\delta\text{SO}_2 - 38 + \delta\text{COOH} - 18 + \gamma\text{CH}_\phi - 10 + \nu\text{NC} - 7 + \nu\text{SN} - 6 + \nu\text{CC}_{\text{COOH}} - 5$	308(1)	$\delta\text{SO}_2 - 48 + \delta\text{COOH} - 19$
71		280(1)	$\delta\text{CH}_{\text{C}\alpha} - 33 + \delta\text{SO}_2 - 20 + \gamma\text{CH}_3 - 7 + \nu\phi - \text{S} - 6$	296(3)	$\delta\text{SO}_2 - 35 + \gamma\text{CC}_{\text{Vi}} - 15 + \delta\text{CH}_{\text{C}\alpha} - 11$
72		266(1)	$\nu\phi - \text{S} - 23 + \delta\text{SO}_2 - 22 + \delta\text{CC}_{\text{Vi}} - 14 + \delta\phi - 6 + \delta\text{CH}_{\text{C}\alpha} - 6$	252(1)	$\nu\phi - \text{S} - 21 + \delta\phi - 18 + \delta\text{SO}_2 - 17 + \delta\text{CH}_{\text{C}\alpha} - 14$
73		232(0)	$\gamma\text{CH}_3 - 56 + \delta\text{CH}_{\text{C}\alpha} - 20 + \delta\text{COOH} - 10$	237(2)	$\gamma\text{CH}_3 - 27 + \delta\text{CH}_{\text{C}\alpha} - 17 + \gamma\text{CC}_{\text{Vi}} - 13 + \delta\text{CC}_{\text{Vi}} - 12$
74		222(0)	$\delta\text{CC}_{\text{Vi}} - 34 + \nu\phi - \text{S} - 10 + \delta\text{SO}_2 - 19 + \delta\phi - 10 + \gamma\text{CH}_\phi - 10 + \delta\text{CS} - 6$	232(0)	$\delta\text{CC}_{\text{Vi}} - 39 + \delta\text{CS} - 10 + \delta\phi - 10$
75		213(0)	$\delta\text{CH}_{\text{C}\alpha} - 38 + \gamma\text{CH}_3 - 29 + \delta\text{COOH} - 16 + \nu\text{SN} - 6$	220(0)	$\gamma\text{CH}_3 - 53 + \delta\text{CH}_{\text{C}\alpha} - 25$
76		192(0)	$\gamma\text{CH}_\phi - 22 + \delta\text{SO}_2 - 23 + \delta\text{CH}_{\text{C}\alpha} - 15 + \delta\text{NH} - 14 + \gamma\phi - 7$	163(2)	$\delta\text{CH}_{\text{C}\alpha} - 18 + \gamma\text{CC}_{\text{Vi}} - 26 + \delta\text{SO}_2 - 15 + \delta\text{CS} - 12 + \delta\text{NH} - 11$
77		135(0)	$\delta\text{CS} - 51 + \delta\text{CC}_{\text{Vi}} - 22 + \delta\text{SO}_2 - 16$	146(0)	$\delta\text{NH} - 25 + \gamma\text{NH} - 23 + \delta\text{SO}_2 - 20 + \delta\text{CH}_{\text{C}\alpha} - 16$
78		122(1)	$\delta\text{NH} - 45 + \gamma\text{CH}_\phi - 12 + \delta\text{SO}_2 - 17 + \gamma\phi - 6 + \delta\text{CH}_{\text{C}\alpha} - 11$	127(0)	$\delta\text{CS} - 37 + \delta\text{SO}_2 - 19 + \delta\text{CC}_{\text{Vi}} - 23$
79		87(1)	$\gamma\text{CH}_\phi - 46 + \gamma\text{CN} - 12 + \gamma\text{NH} - 10 + \gamma\text{SN} - 7 + \gamma\text{COOH} - 6 + \gamma\text{CC}_{\text{Vi}} - 6 + \gamma\text{CS} - 6$	88(0)	$\gamma\text{CS} - 37 + \gamma\text{CN} - 15 + \gamma\text{CC}_{\text{Vi}} - 15 + \gamma\text{COOH} - 10$
80		59(0)	$\gamma\text{COOH} - 89 + \gamma\text{CH}_\phi - 8 + \delta\text{SO}_2 - 6$	59(0)	$\gamma\text{COOH} - 84 + \gamma\text{CS} - 11$
81		44(0)	$\gamma\text{CC}_{\text{Vi}} - 37 + \gamma\text{CS} - 31 + \gamma\text{SN} - 10 + \gamma\text{NH} - 7 + \gamma\text{COOH} - 5$	31(0)	$\gamma\text{CC}_{\text{Vi}} - 56 + \gamma\text{SN} - 19$
82		31(0)	$\gamma\text{SN} - 47 + \gamma\text{CS} - 23 + \gamma\text{NH} - 9 + \gamma\text{CN} - 6 + \gamma\text{CH}_\phi - 6$	30(0)	$\gamma\text{CS} - 63 + \gamma\text{SN} - 19$
83		27(0)	$\gamma\text{CC}_{\text{Vi}} - 44 + \gamma\text{CS} - 38 + \gamma\text{CH}_\phi - 14 + \gamma\text{CN} - 6$	20(0)	$\gamma\text{CN} - 85 + \gamma\text{SN} - 15$
84		17(0)	$\gamma\text{CN} - 81 + \gamma\text{CH}_\phi - 8$	16(0)	$\gamma\text{CS} - 39 + \gamma\text{CC}_{\text{Vi}} - 26 + \gamma\text{SN} - 25$

Ph—phenyl ring; ν —stretching; δ —in-plane deformation; γ —out-of-plane deformation; τ —torsion. Potential energy distribution is given in the assignment column.

The theoretical chemical shift values were calculated by B3LYP method using 6-311+g(*d,p*) basis set GIAO model (scale number = 0.9614). Then, the results showed that the predicted proton chemical shifts were in good agreement with the experimental data for ASS which was represented in. The RMS error between observed and calculated $^1\text{H-NMR}$ is 0.31. The small differences between experimental and calculated vibrational modes are observed. This is due to the fact that experimental results belong to the solid phase and theoretical calculations belong to the gaseous phase.

Molecular Electrostatic Potential

Molecular electrostatic potential (MEP) is as a significant tool to predict the electrophilic and nucleophile attacks for the biological interactions. The MEP of the title compound optimized geometry was calculated by CAM-B3LYP method Aug-cc-pVDZ basis set. As it can be observed from the Fig. 6. As can be seen from the MEP map of the *N*-(alanine) *p*-styrene sulfonamide the negative region is mainly over the electro negative oxygen atoms. The maximum positive region is localized on the phenyl rings.

Frontier Molecular Orbital Analysis

Investigation of the HOMO and the LUMO is important in a molecule as a ligand. Soft systems are large and highly polarizable, while hard systems are relatively small and much less polarizable. For understanding various aspects of the drugs design and their characteristic, several new chemical reactivity descriptors have been proposed. The LUMO energy explains the ability to accept an electron and the HOMO energy is related to the ability to donate an electron. Both the HOMO and the LUMO, play a significant role in the electrical properties and chemical activities in the compound. The HOMO and the LUMO orbital energy are important parameters to predict the chemical properties of a compound. The HOMO and the LUMO orbital energy of ASS are calculated at the

Table 4. Experimental and calculational results related to $^1\text{H NMR}$ of ASS (*N* is hydrogen number)

<i>N</i>	Exp.	Cal.	<i>N</i>	Exp.	Cal.
8, 9	7.75	7.60	17	5.42	5.22
10, 11	7.59	7.16	20	4.7	4.81
19	6.77	6.53	26	3.97	4.20
18	5.92	5.94	28, 29, 30	1.42	0.86

Observed and computed $^1\text{H NMR}$ chemical shifts with their assignments.

CAM-B3LYP method Aug-cc-pVDZ basis set. The energy values are, $E_{\text{HOMO}-1} = -9.18$, $E_{\text{HOMO}} = -8.32$, $E_{\text{LUMO}} = -0.88$, $E_{\text{LUMO}+1} = 0.07$ eV. The energy difference between the HOMO and the LUMO is 7.44 eV. The energy of HOMO and the LUMO orbitals of the ASS is negative showing that this compound is stable and does not decompose spontaneously into its elements. The energy gap = HOMO – LUMO = 7.44 eV. According to Parr et al. [34], the larger the HOMO–LUMO energy gap, the harder the molecule. A molecule with a high energy gap is less polarizable, it has high kinetic stability and it is termed as a hard molecule. The hardness (weakly polarizable) can be explained as the resistance towards the deformation of electron cloud and polarization of chemical systems during the chemical process. The chemical hardness is a useful concept for predicting the behavior of chemical systems and is related to the stability of a chemical system. By using the HOMO and the LUMO orbital energies, the ionization energy and electron affinity can be calculated as: $I = -E_{\text{HOMO}} = 8.32$ and $A = -E_{\text{LUMO}} = 0.88$ eV. The global hardness η and chemical potential μ are given by using the relation $\eta = (I - A)/2 = 3.72$ eV and $\mu = -(I + A)/2 = -4.60$ eV global electrophilicity = $\mu^2/2\eta = 2.84$ eV. The atomic orbital components of the frontier molecular orbital are shown in Fig. 7.

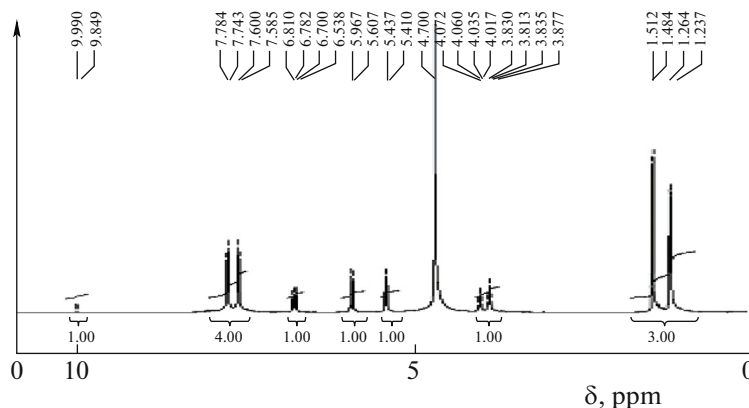


Fig. 5. The experimental $^1\text{H-NMR}$ of ASS.

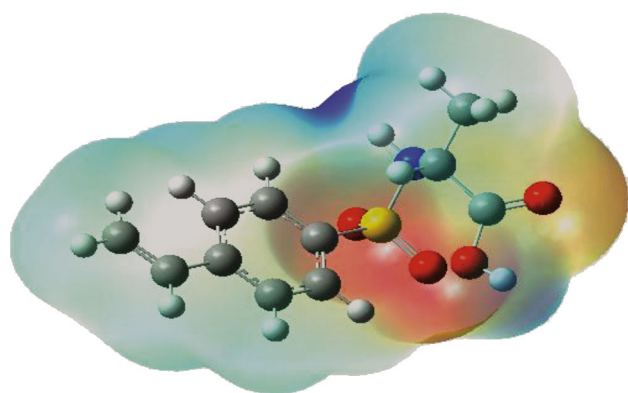


Fig. 6. (Color online) MEP plot of *N*-(alanine) *p*-styrene sulfonamide.

Molecular Docking Studies on DNA and BSA

We decided to perform molecular docking simulation of the title compound against the 3D crystal structure of DNA and BSA were obtained from Protein Data Bank (PDB ID: 423D, 4F5S) respectively. Molecular docking is a significant investigation method to understand the ligand-receptor interactions. The ligand was prepared for docking by using CAM-B3LYP method Aug-cc-pVDZ basis set. The active sites of the DNA and BSA were defined to include residues of the active site within the grid box size of $38 \times 30 \times 24 \text{ \AA}$ for DNA and $82 \times 58 \times 62 \text{ \AA}$ for BSA with a grid-point spacing of 1.00 \AA were applied. Amongst the docked conformations, the best scored conformation predicted by AutoDock scoring function were visualized for ligand-DNA and ligand-

BSA interactions in Ligplot and Ligplus software. The docking study on the PSS-DNA system showed that the ASS places in the major groove of DNA (A). Also, the molecular docking study of BSA showed that the ASS places in the binding pocket of BSA(B).

The resulting docking in which the ligand binds into the DNA creates two hydrogen bonds (Fig. 8). The first hydrogen bond is between the N_{NH} of ASS and Dg22 (3.22 \AA). The second hydrogen bond is between O_{SO_2} of ASS with Dg22 (2.83 \AA). There are hydrophobic contacts between the carbon atoms of phenyl ring and Da5. The ligand binds into the BSA and creates four hydrogen bonds (Fig. 8), viz. Three hydrogen bond are between the O_{CO_2} and Arg 409, Phe 487, Tyr 410 ($3.29, 3.18, \text{ and } 3.09 \text{ \AA}$, respectively). The fourth hydrogen bond is between O_{SO_2} of ASS with Tyr 410 (3.09 \AA). In addition, there are hydrophobic contacts between the carbon atoms of the ASS with Leu 452, Leu 429, Phe 402, Val 432, Leu 386, Ser 488, Lys 413, and Asn 390. The binding free energy (ΔG° , kcal mol^{-1}) -6.5 for DNA and -7.4 for BSA are predicted for the best conformation of the ligand. The values of ΔG° indicate a high binding affinity between DNA and BSA separately with the ASS.

The Disk Diffusion Method

A microbial suspension (1 mL) *Staphylococcus aureus* and *Escherichia coli* was spread separately over the surface of agar plate, which were then incubated for 24 h at 37°C in an autoclave. Inhibitory zone values (diameter of inhibition) from disk diffusion tests and

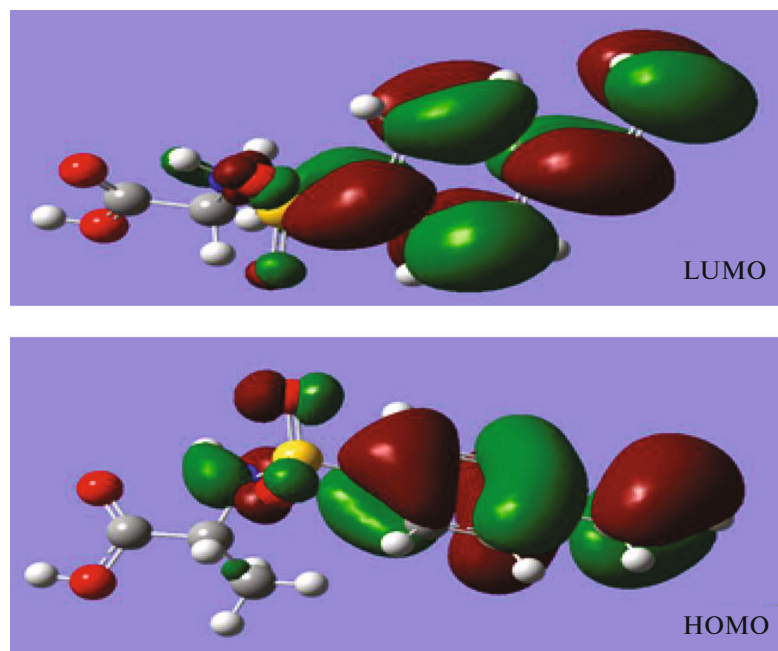


Fig. 7. (Color online) HOMO and LUMO plots of *N*-(alanine)-*p*-styrene sulfonamide.

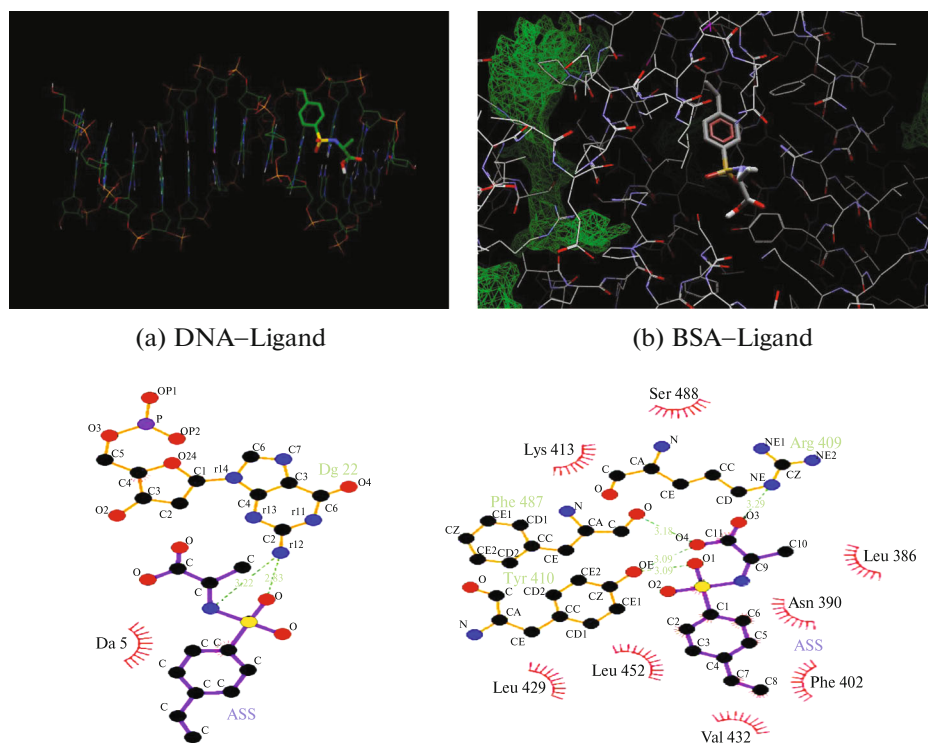


Fig. 8. (Color online) (a) Perspective of molecular docking of ligand with the major groove side of DNA. (b) The ASS docked in the binding pocket of BSA. The non-covalent interactions and hydrophobic forces across the binding interface of Ligand–DNA in the left and ligand–BSA in the right (H bonds are shown by dotted lines).

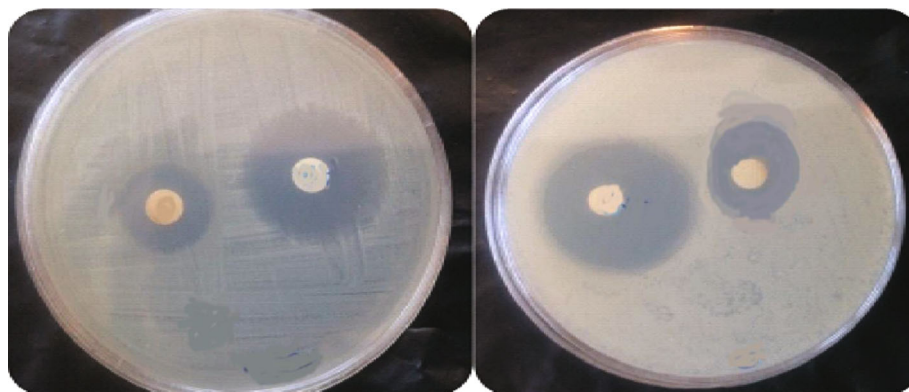


Fig. 9. (Color online) The growth inhibition ring observed for ligand in *S. aureus* in the right and *E. coli* in the left.

growth inhibition ring for ASS are reported in Table 5 and Fig. 9.

The results of this assay can be showed that both of *Staphylococcus aureus* and *Escherichia coli* are sensitive to *N*-(alanine)–*p*-styrene sulfonamide but *Staphylococcus aureus* more sensitiveness to the compounds.

Table 5. Inhibitory zone values (*d* is diameter of zone inhibition) from disk diffusion tests

Compound	Bacteria	<i>d</i> , mm
<i>N</i> -(Alanine) sulfonamide	<i>E. coli</i>	18
<i>N</i> -(Alanine) sulfonamide	<i>S. aureus</i>	19

CONCLUSIONS

We report the new compound of based-alanine sulfonamide. The molecular geometry and structural parameters of the title compound were calculated using CAM-B3LYP method Aug-cc-pVDZ basis set. ^1H NMR spectrum obtained using B3LYP/6-311+g(*d,p*), was compared with experimental results. An analogous comparison was made for infrared spectra. This research leads us to find that the theoretical results are in good agreement with the experimental data. The molecular electrostatic potential and frontier molecular orbital analysis indicate that the ASS can be designed for the new catalyst due to its properties. The

biological investigation results suggest that ASS can be used for the design and synthesis of new based-drug materials.

FUNDING

We would like to thank Lorestan University for its financial support.

REFERENCES

- N. N. Al-Mohammed et al., *Molecules* **18**, 11978 (2013).
- S. S. Stokes et al., *Bioorg. Med. Chem. Lett.* **22**, 7019 (2012).
- P. Zoumpoulakis et al., *Bioorg. Med. Chem. Lett.* **20**, 1569 (2012).
- S. Br et al., *J. Med. Chem.* **23**, 9855 (2014).
- C. T. Supuran et al., *Mini. Rev. Med. Chem.* **4**, 189 (2004).
- M. F. Mohamed et al., *Appl. Biochem. Biotech.* **168**, 1153 (2012).
- X. Jin et al., *Eur. J. Med. Chem.* **56**, 203 (2012).
- F. M. Awadallah et al., *Eur. J. Med. Chem.* **96**, 425 (2015).
- M. M. Ghorab, M. Ceruso, M. Alsaïd, Y. M. Nissan, R. K. Arafâ, and C. T. Supuran, *Eur. J. Med. Chem.* **87**, 186 (2014).
- A. Kamal et al., *Bioorg. Med. Chem. Lett.* **20**, 4865 (2010).
- K. V. Sashidhara et al., *Bioorg. Med. Chem. Lett.* **20**, 7205 (2010).
- M. Mirian et al., *Iran. J. Pharm. Res.* **10**, 741 (2011).
- R. Levine et al., *Diabetes* **6**, 263 (1957).
- S. Riaz et al., *Bioorg. Chem.* **63**, 64 (2015).
- M. Adib et al., *Tetrahedron Lett.* **51**, 5646 (2010).
- A. Mascarello et al., *Eur. J. Med. Chem.* **86**, 491 (2014).
- A. Alsughayer et al., *J. Biomater. Nanobiotechnol.* **2**, 144 (2011).
- N. D. Reddy et al., *Chem.-Biol. Interact.* **253**, 112 (2016).
- R. Pingaew et al., *Eur. J. Med. Chem.* **103**, 446 (2015).
- A. Yari, E. Mehdipour, and M. Karami, *J. Fluoresc.* **24**, 1415 (2014).
- E. Mehdipour et al., *J. Phosphorus, Sulfur, Silicon Rel. Elem.* **190**, 1588 (2015).
- N. Yada et al., *J. Polym. Sci., Part A* **3**, 2229 (1968).
- M. J. Frisch, H. B. S. G. W. Trucks, G. E. Scuseria, M. A. Robb, J. R. Cheeseman, G. Scalmani, V. Barone, B. Mennucci, G. A. Petersson, H. Nakatsuji, M. Caricato, X. Li, H. P. Hratchian, A. F. Izmaylov, J. Bloino, et al., *Gaussian 09, Revision C.01* (Gaussian Inc., Wallingford, CT, 2010).
- A. D. Becke, *J. Chem. Phys.* **98**, 5648 (1993).
- H. Tavakol and F. Keshavarzipour, *Struct. Chem.* **26**, 1049 (2015).
- O. Trott et al., *J. Comput. Chem.* **31**, 455 (2010).
- M. J. Nowak and L. Lapinski, *Vibrat. Spectrosc.* **49**, 43 (2009).
- A. Lagunin, A. Stepanchikova, D. Filimonov, and V. Poroikov, *Bioinformatics* **16**, 747 (2000).
- A. Vina, *J. Comput. Chem.* **31**, 455 (2010).
- G. M. Morris, D. S. Goodsell, R. S. Halliday, R. Huey, W. E. Hart, and R. K. Belew, *J. Comput. Chem.* **19**, 1639 (1998).
- R. Huey et al., *J. Comput. Chem.* **28**, 1145 (2007).
- A. C. Wallace et al., *J. Med. Chem.*, 127 (1996).
- NCCLS, Methods for dilution antimicrobial susceptibility test for bacteria that grow aerobically, M7-A4 (1997).
- R. G. Parr et al., *J. Am. Chem. Soc.* **121**, 1922 (1999).